

## *A Study of Anisotropic Workhardening*

Norio HOSOKAWA\* and Yoichi KODERA\*\*

(Received September 16, 1972)

### Synopsis

This paper deals with the stress-strain curves of single crystal and polycrystal considering the workhardening and the anisotropy which is due to the difference of workhardening on each slip system.

The results obtained are summarized as follows:

- 1) The equations of workhardening on each slip system are derived according to the dislocation theory.
- 2) And it is found that the stress-strain curves of Cu single crystal and polycrystal calculated by using the workhardening equation with proper coefficients agree well with the experimental values.

### 1. Introduction

Recently, it has been possible to analyze the stresses and the strains of the complicated shaped bodies applying to finite element method. It is known that this method has a good accuracy when the body is divided to small elements<sup>(1)</sup> and the equations between the stresses and the strains are well known as Hooke's law in elastic deformation. But, in plastic deformation, the phenomena in which the stress-strain curves are changed by preworks<sup>(2)</sup> are not yet explained completely, therefore, the equations in the region of plastic deformation cannot be represented in good accuracy. So the equations be-

---

\* Department of Mechanical Engineering

\*\* Graduate School of Mechanical Engineering

tween the stresses and the strains in plastic deformation have to be made clear, for analyzing the stresses and strains in plastic deformation of the complicated shaped body.

Generally, the all metals for practical using are polycrystal and the mechanism of plastic deformation is the slip as single crystal. Although the behavior of the plastic deformation of single crystal is well known in crystallography and the dislocation theory,<sup>(3)</sup> the property of polycrystal differs from the average one of single crystal because a grain in polycrystal is affected by the neighbouring grains.

In this paper, the equations between the stresses and strains of single crystal and polycrystal are studied mainly considering the anisotropic workhardening.

## 2. Theoretical analysis and results

### 2.1 Workhardening in slip deformation

Plastic deformation of metal occurs by the movement of dislocations. The obstacles for moving dislocation are impurities, alloying elements, Peierls-Nabarro force and the other dislocations, etc. Since the obstacles on the workhardening must increase with deformation, the main factor is considered the interaction with the other dislocations. Fig.1 shows the

relation between moving dislocation on a slip plane and forest dislocations which intersect with this slip plane and which are obstacles to this moving dislocation. Force on the dislocation line of length  $l$  is given as  $(\tau - \tau_0)bl$  under applied shear stress  $\tau$  in the slip direction on the slip plane, the frictional stress  $\tau_0$

and Bergers vector  $b$ . And this force must overcome the force  $F$  for cutting the obstacles in order that the dislocation can pass through the forest dislocations. Therefore the minimum applied stress for movement of the dislocation is as follows:

$$\tau = \tau_0 + \frac{F}{bl} \quad (1)$$

Also, when the dislocation moves among the dislocations of the same slip system, maximum force in a unit dislocation length subjected by other dislocations is  $\mu b^2 / 8\pi(1-\nu)h$ ,<sup>(3)</sup> as in Fig.2.

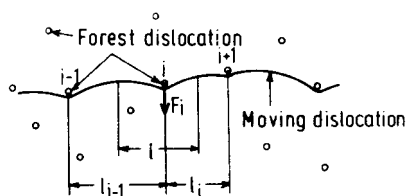


Fig.1 The shape of moving dislocation affected by the forest of dislocations

Therefore, in order that the dislocation can pass through the dislocations, the applied stress needs at least

$$\tau = \tau_0 + \frac{\mu b^2}{8\pi(1-\nu)h} \quad (2)$$

where  $\mu$  and  $\nu$  represent shear modulus and Poisson's ratio respectively.

Consequently, the average values  $\bar{l} = K_1 / \sqrt{\rho_f}$  or  $\bar{h} = K_2 / \sqrt{\rho_p}$  are often adopted in order to estimate the flow stress where  $\rho_f$  and  $\rho_p$  represent the density of forest dislocations and the density of dislocations on the parallel slip plane respectively, and  $K_1$  and  $K_2$  are constants that are nearly 1. So, from eq.(1) and eq.(2), following equation is obtained:

$$\tau = \tau_0 + \frac{\tau}{K_1 b} + \frac{\mu b^2}{8\pi K_2 (1-\nu)h} \quad (3)$$

But  $l$  has the distribution and there exists  $l$  which is longer than  $\bar{l}$ . Therefore, the dislocation can move even when the stress which is less than that given in eq.(3) is exerted.

Let's assume that the dislocations are distributed at random in the grain. So, the probability density  $\alpha$  which  $(l_{i-1} + l_i)/2$  is  $l$  is

$$\alpha = 2K_3 \rho_f \exp(-K_3 \rho_f l^2) \quad (4)$$

where  $K_3$  is constant, and from the definition of the probability density

$$\int_0^{\infty} \alpha dl = 1 \quad (5)$$

Further, let the number of the nodes between the moving dislocations and the forest dislocations be  $n$ , and the density of the moving dislocations are obtained as:

$$\rho_m = \int_0^{\infty} n l \cdot \alpha dl = n \bar{l} \quad (6)$$

The incremental shear strain  $dY$  is

$$dY = n \int_{l_c}^{\infty} b \cdot ds \cdot \alpha dl \quad (7)$$

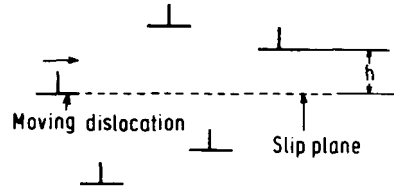


Fig.2 Relation between the moving dislocation and other dislocations on the same slip plane

where  $l_c$  represents the smallest value of  $l$  that the moving dislocation passes through, and from eq.(1)

$$l_c = \frac{F}{b(\tau_c - \tau_0)} \quad , \quad (8)$$

and  $ds$  represents the area which the dislocation sweeps after it passes through one node and is considered to be in proportion to  $vl$  ( $v$  is the velocity of moving dislocation) or  $l^2$  in according to strain rate. Substituting eq.(4), eq.(6) and eq.(8) into eq.(7) and putting  $x = \sqrt{K_3 \rho_f} l$  ,

$$dY = K_4 b \rho_m v \int \frac{F \sqrt{K_3 \rho_f}}{b(\tau_c - \tau_0)} x^2 \exp(-x^2) dx \quad (ds = K_4 vl) \quad (9)$$

$$dY = \frac{2K_5 b \rho_m}{K_3 \sqrt{\rho_f}} \int \frac{F \sqrt{K_3 \rho_f}}{b(\tau_c - \tau_0)} x^3 \exp(-x^2) dx \quad (ds = K_5 l^2) \quad (9')$$

$dY$  is expressed as the function of  $(\tau_c - \tau_0)$  by integrating eq.(9), and the relation between  $dY$  and  $(\tau_c - \tau_0)$  is shown in Fig.3, and the result in eq.(9') is very close to that in eq.(9).

This curve is approximated to the one point chain line in Fig.3 except low strain rate and high strain rate.

$$\tau_c - \tau_0 = \frac{F \sqrt{K_3 \rho_f}}{b} \left( \frac{KdY}{\rho_m v} + 0.5 \right) \quad (10)$$

But, generally, the distribution of dislocations are not always at random and they often tangle or pile up.<sup>(4)</sup> The relation is therefore expressed qualitatively as the broken line and is approximated to the two point chain line except low strain rate and high strain rate, as in Fig.3.

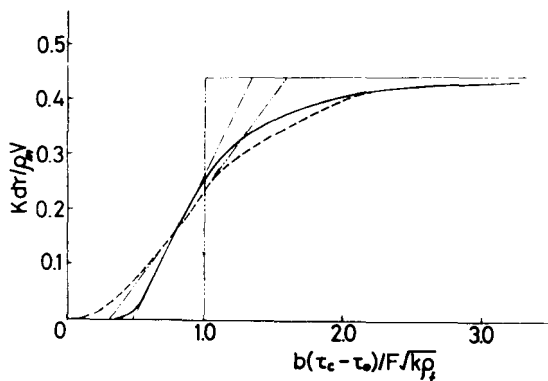


Fig.3 Relation between the shear strain and the flow stress

And the approximate equation is:

$$\tau_c - \tau_o = \left( \frac{A d\gamma}{\rho_m v} + B \right) F \sqrt{\rho_f} \quad (11)$$

where A and B are constants and the relation between  $d\gamma$  and  $(\tau_c - \tau_o)$  in any distribution of dislocations is approximated by determining proper A and B. The relation when  $l = \bar{l}$  in the dislocation theory as described before coincides when  $A = 0$  in eq.(11). And all cases are represented by eq.(11).

$\rho_m$  is the unknown value, but it can be written approximately:

$$\rho_m = p + q \rho_p \quad (12)$$

where p and q are constants which change by materials.

Substituting eq.(12) into eq.(11),

$$\tau_c - \tau_o = \left( \frac{A d\gamma}{p + q \rho_p} + B \right) F \sqrt{\rho_f} \quad (13)$$

Until now, the Primary slip system and one other slip system are considered. But there are 12 slip systems in face-centered cubic metal and 48 in body-centered cubic metal. So, the general case must be considered. Let the density of dislocations on j th slip system be  $\rho_j$  and k th slip system be active. The dislocations on each slip system interact each other, but the force of interaction is different by the combination of slip systems. So, the three equations are obtained as follows:

$$\tau_c^k = \tau_o + \left( \frac{A d\gamma^k}{p + q \rho_p} + B \right) \cdot \sum_j H_{kj} \sqrt{\rho_j} \quad (14)$$

$$\tau_c^k = \tau_o + \left( \frac{A d\gamma^k}{p + q \rho_p} + B \right) \cdot \sqrt{\sum_j H_{kj} \rho_j} \quad (15)$$

$$\tau_c^k = \tau_o + \left( \frac{A d\gamma^k}{p + q \rho_p} + B \right) \cdot \left( \sum_j H_{kj} \rho_j \right)^{3/2} / \left( \sum_j \frac{H_{kj} \rho_j}{F_j} \right) \quad (16)$$

Since it is reported that the density of dislocations  $\rho_j$  is in proportion to the shear strain  $\gamma_j$  by experiments of single crystal and polycrystal, the shear stress-shear strain equations are as:

$$\tau_c^k = \tau_o + \left( \frac{A d\gamma^k}{p + q (\gamma^k + \gamma_{oj})} + B \right) \cdot \sum_j H_{kj} \sqrt{\gamma_j + \gamma_{oj}} \quad (17)$$

$$\tau_c^k = \tau_o + \left( \frac{A d\gamma^k}{p + q (\gamma^k + \gamma_{oj})} + B \right) \cdot \sqrt{\sum_j H_{kj} (\gamma_j + \gamma_{oj})} \quad (18)$$

$$\tau_c^k = \tau_o + \left( \frac{A d\gamma^k}{p+q(\gamma^k + \gamma_{oj})} + B \right) \cdot \left( \sum_j H_{kj} (\gamma_j + \gamma_{oj}) \right)^{3/2} / \left( \sum_j \frac{H_{kj} (\gamma_j + \gamma_{oj})}{F_j} \right), \quad (19)$$

where  $\gamma_{oj}$  is the strain into which the density of dislocations at the initial state is converted and  $H_{kj}$  is a constant depended on  $k$  th and  $j$  th slip systems.

## 2.2 The stress-strain curves of single crystal

Let the coordinate  $O-x_1x_2x_3$  be in crystal axis and let the direction cosines of the coordinate axis  $X_i$  which is fixed on the specimen be  $(l_i, m_i, n_i)$  ( $i=1,2,3$ ). And the resolved shear stress  $\tau^k$  on the  $k$  th slip system is related to the applied stress  $\sigma_{ij}$  as:

$$\tau^k = \sum_i \sum_j (l_i p_1^k + m_i q_1^k + n_i r_1^k) (l_j p_2^k + m_j q_2^k + n_j r_2^k) \sigma_{ij}, \quad (20)$$

where  $(p_1^k, q_1^k, r_1^k)$  and  $(p_2^k, q_2^k, r_2^k)$  are the normal direction of slip plane and slip direction of  $k$  th slip system.

And the components of strain in plastic deformation are expressed as follows:

$$d\epsilon_{ij} = \frac{1}{2} \sum_k ((l_i p_1^k + m_i q_1^k + n_i r_1^k) \cdot (l_j p_2^k + m_j q_2^k + n_j r_2^k) + (l_j p_1^k + m_j q_1^k + n_j r_1^k) \cdot (l_i p_2^k + m_i q_2^k + n_i r_2^k)) d\gamma^k, \quad (21)$$

where  $d\gamma^k$  is the incremental shear strain of  $k$  th slip system.

In the slip systems that  $\tau^k$  in eq.(20) reaches the value  $\tau_c^k$ , the slip occurs, and in another slip systems, the slip does not occurs. Therefore, following condition can be obtained:

$$\begin{aligned} d\gamma^k &\geq 0, & \text{when } \tau^k &= \tau_c^k, \text{ or} \\ d\gamma^k &= 0, & \text{when } \tau^k &< \tau_c^k. \end{aligned} \quad (22)$$

## 2.3 Comparison between the calculated results and the experimental results in single crystal

Even if any equation of eq.(17), eq.(18) and eq.(19) is used as the approximate equation of workhardening, the stress-strain curves can be represented by choosing the suitable values of  $A$ ,  $B$ ,  $p$ ,  $q$  and

$H_{kj}$ . For example, the results calculated by using eq.(17) are reported.

Parameters A and B which indicate the distribution of dislocation and the density of moving dislocations are not completely made clear Therefore the coefficients must be determined by comparison with experimental data in single crystal , although  $H_{kj}$  can be determined from the value reported by many workers.<sup>(5)</sup>

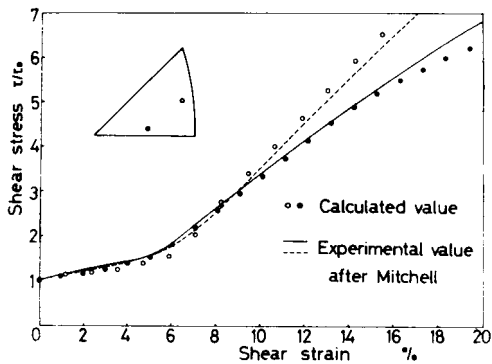


Fig.4 Comparison between calculated flow stress and experimental one of Cu single crystal after Mitchell

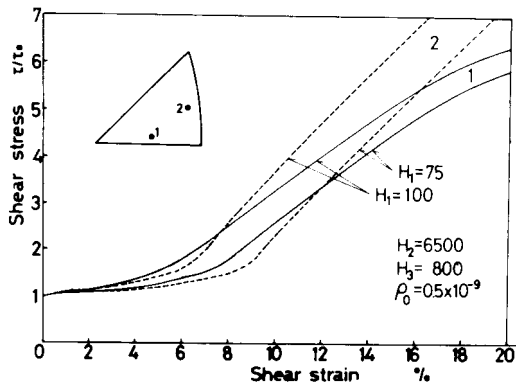


Fig.5 The effect of  $H_1$  on the resolved shear stress-shear strain curve

And  $AH_{kj}/p$  are classified into the following three groups, that is,  $H_1$ ,  $H_2$  and  $H_3$ .

$H_1$  is the coefficient which represents the interaction of dislocations on the same slip plane,  $H_2$  is the coefficient depended on the combination of slip planes in which Lomer-Cottrell dislocations are formed, and  $H_3$  is the other coefficient.

And the coefficients of Cu single crystal are obtained as follows by comparison with the experimental values which was measured by Mitchell<sup>(6)</sup> in the two orientations in the stereographic triangle in Fig.4.

$$\begin{aligned}
 B &= 0, \quad q = 0 \\
 \gamma_0 &= 0.5 \times 10^{-9} \\
 H_1 &= 100 \text{ Kg/mm}^2 \\
 H_2 &= 6500 \text{ Kg/mm}^2 \\
 H_3 &= 800 \text{ Kg/mm}^2.
 \end{aligned}$$

In order to obtain the stress-strain curves of other face centered cubic metals, the effect of the coefficients must be known.

Fig.5 shows the shear stress-shear strain curves when  $H_1$  is changed. When  $H_1$  becomes larger, the gradient of the

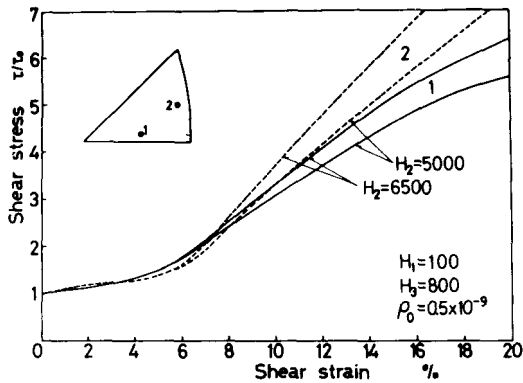


Fig. 6 The effect of  $H_2$  on the resolved shear stress-shear strain curve

first stage becomes larger and the strain becomes less. But the gradient of the second stage does not change so much.

Fig. 6 shows the shear stress shear strain curves when  $H_2$  is changed.  $H_2$  affects mainly the gradient of the second stage. When  $H_2$  becomes larger, the gradient of the second stage becomes larger.

Fig. 7 shows the shear stress-shear strain curves when  $H_3$  is changed. This also exerts an influence upon the gradient

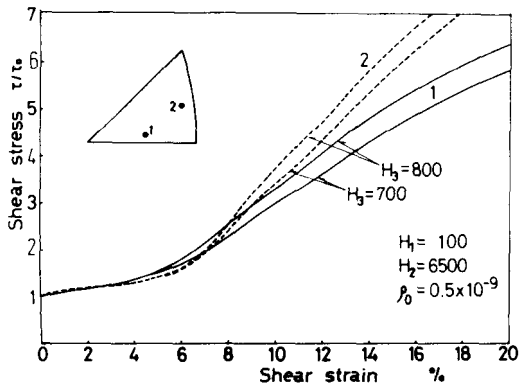


Fig. 7 The effect of  $H_3$  on the resolved shear stress-shear strain curve

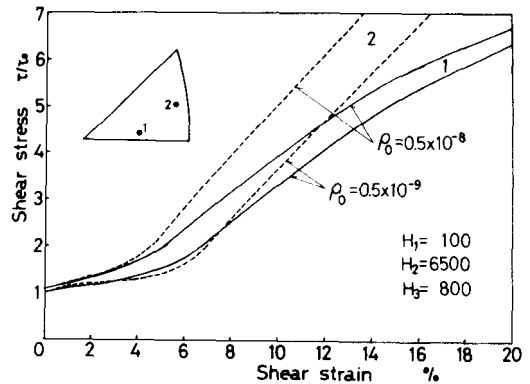


Fig. 8 The effect of  $\rho_0$  on the resolved shear stress-shear strain curve

of the second stage.

Fig. 8 shows the effect of  $\rho_0$ , and  $\rho_0$  controls the yield strength and the length of the first stage.

Considering the effect of each coefficient described above, the more suitable coefficients can be obtained although they interact each other.



## 2.4 Effect by neighbouring grains

Effect by neighbouring grains have to be made clear, in order to know the deformation behavior of each grain in polycrystal, but it is not so easy to solve this problem. Therefore the following a few models are considered for deformation.

In order to solve eq.(20) and eq.(21), 6 components must be known as a boundary condition in 12 components of  $\sigma_{ij}$  and  $d\varepsilon_{ij}$ . But, generally, these values in a grain are unknown. Therefore it is assumed that the strains of each grain are equal to the mechanical strains of specimen in according to Taylor's model.<sup>(7)</sup> However, if there are given components in stresses and strains, their values are used as boundary conditions instead of the above assumption.

a) In the case that tri-axial stress is applied in specimen, boundary conditions are as follows:

$$d\varepsilon_{ij} = dE_{ij} , \quad (23)$$

where  $dE_{ij}$  is the mechanical strain of specimen.

b) In the case that plane stress is applied in specimen:

$$\begin{aligned} \sigma_{33} = \sigma_{23} = \sigma_{13} = 0 , \quad d\varepsilon_{11} = dE_{11} , \quad d\varepsilon_{22} = dE_{22} , \\ d\varepsilon_{12} = dE_{12} . \end{aligned} \quad (24)$$

Substituting these conditions and solving eq.(20) and eq.(21), unknown components of stresses and strains in a grain affected by neighbouring grains are determined.

## 2.5 The stress-strain curves of polycrystal

Polycrystal consists of many grains and there exist grain boundaries between them. The strength in a grain is determined by the method described as above. The strength of their boundaries are <sup>(8)</sup> however not determined although many works and theory are reported. But the volume of grain boundary is not so larger than that of grain. Therefore the effect of grain boundary can be neglected even if they are so different from the strength of grain.

Representating the relation between the coordinate  $O-x_1x_2x_3$  and  $O-X_1X_2X_3$ ,  $\phi$ ,  $\theta$  and  $\psi$  are introduced. That is,  $\phi$  is an angle between  $x_1$  axis and the projective direction of  $X_1$  axis on the plane  $x_1x_2$ ,  $\theta$  is an angle between  $x_1$  axis and the projective direction of  $X_1$  axis on the plane  $x_1x_3$ , and  $\psi$  is an angle between  $X_2$  axis and the normal of the plane which contains both  $x_3$  axis and  $X_1$  axis.

$\sigma_{ij}(\phi, \theta, \psi)$ ,  $d\varepsilon_{ij}(\phi, \theta, \psi)$  and  $f(\phi, \theta, \psi)$  represent the stresses, the strains of a grain having this of grains having this orientation, respectively. In this  $f(\phi, \theta, \psi)$ , the change of area on a spherical surface divided by  $d\phi$  and  $d\theta$  with  $\phi$  and  $\theta$  in integrating the following equations is taken into account.

So, the average stresses ( $S_{ij}$ ) and strains ( $dE_{ij}$ ) are written as follows:

$$S_{ij} = \iiint \sigma_{ij}(\phi, \theta, \psi) \cdot f(\phi, \theta, \psi) \, d\psi d\phi d\theta. \quad (25)$$

$$dE_{ij} = \iiint d\varepsilon_{ij}(\phi, \theta, \psi) \cdot f(\phi, \theta, \psi) \, d\psi d\phi d\theta. \quad (26)$$

## 2.6 Comparison between the calculated results and the experimental results in polycrystal

The stress-strain curves of polycrystal in the tri-axial stress condition and in the plane stress condition are calculated by using the same coefficients that is used in the calculation of Cu single crystal. The calculated values agree well with the experimental values, as shown in Fig.9. Where the experimental values are obtained by Konuma<sup>(9)</sup> and are converted into  $\sigma/\tau_0$  by multiplying the measured yield stress by  $3.08/\sigma_y$ .

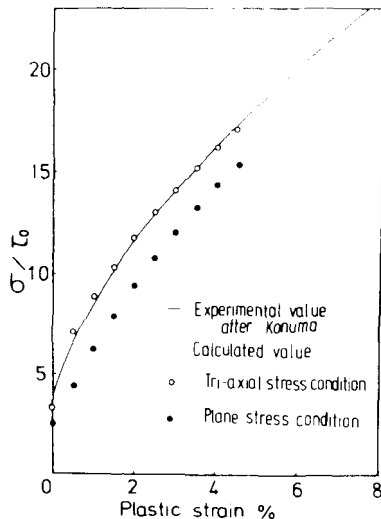


Fig.9 Comparison between the calculated stress-strain curve and the experimental one of Cu polycrystal after Konuma

Black dots in Fig.9 represent the calculated values in the plane stress condition. And the stress in the plane stress condition are less than that in the tri-axial stress condition. Therefore the fact that the compressive residual stress come into existence on the surface layer of plastic elongated specimen is explained qualitatively because the surface layer is in plane stress condition.

### 3. Discussion

The stress-strain curves of Cu at the room temperature are approximated well when both B and q are zero as described before. The effect of A, B, p and q are discussed.

Approximate eq.(3) which is used often in studies of the dislocation theory is the equation putted  $A = 0$  in eq.(14). Fig.10 shows the schematic stress-strain curve when  $A = 0$ . When  $H_2 > H_1$ , secondary slip system does not act as shown by the solid line. When  $H_2 < H_1$ , there is an inflection point and the secondary slip system begins to act at this point as shown by the broken line.

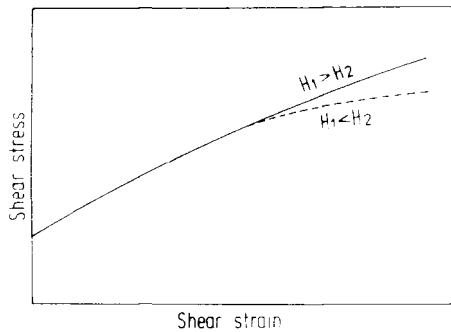


Fig.10 Influence of A on resolved shear stress-shear strain curve

Let A be constant and the value B be changed. As in Fig.11, the broken line represents the diagram when  $B = 0$ . And the gradient of easy glide become larger at the end of easy glide become larger when B becomes larger as shown by the solid line.

When  $p = 0, q \neq 0$ , the stress become lower just after yield point and the length of easy glide is long as shown by the solid line in Fig.12.

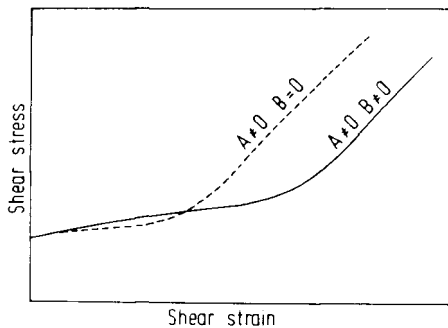


Fig.11 Influence of B on resolved shear stress-shear strain curve

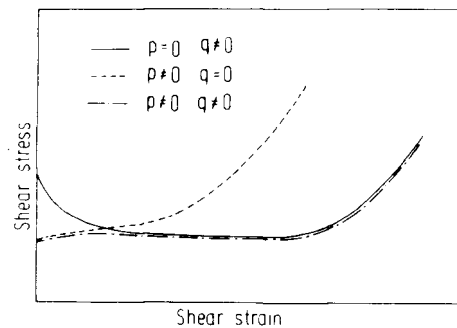


Fig.12 Influence of p and q on resolved shear stress-shear strain curve

On the contrary, when  $p \neq 0$  and  $q = 0$ , there is no drop in stress after yield point as shown by the broken line in Fig. 12. And when  $p \neq 0$  and  $q \neq 0$ , the diagram becomes near to the broken line because  $q\beta_p$  is nearly zero in the early stage, and then becomes near to the solid line because  $q\beta_p$  becomes large when deformation is large as shown in Fig. 12.

#### 4. References

- (1) Zienkiewicz, O. C., Cheung, Y. K.: "The finite element method in structural and continuum mechanics" McGraw-Hill, (1967), 1.
- (2) Tosawa, Y., Nakamura, M.: J. JSME, 75, (1971), 541.
- (3) Hashiguchi, R. et. al.: "Dislocation theory -Application to metallograph-" Maruzen, (1971), 49.
- (4) Essmann, U.: Acta Met., 12, (1964), 1467.  
Bailey, J. E., Hirsch, P. B., Phil. Mag., 5, (1960), 485.  
Steeds, J. W.: Proc. Roy. Soc., A 292. (1966), 343.
- (5) Saada, G.: Acta Met., 8, (1960), 841.  
Carrington, W., Hale, K. F., McLean, D.: Proc. Roy. Soc., A 259, (1959), 1.  
Foreman, A. J. E., Makin, M. J.: Phil. Mag., 4, (1966), 911.
- (6) Mitchell, T. E., Thronton, P. R.: Phil. Mag., 1, (1963), 1136.
- (7) Taylor, G. I.: J. Inst. Met., 62, (1938), 307.
- (8) Takeuchi, T.: J. Japan Soc. Tech. Plas., 11, (1970), 457.
- (9) Konura, M.: J. JIM, 29, (1965), 12.